SIGMA PHASE IN THE TERNARY SYSTEMS CHROMIUM-COBALT-COPPER AND CHROMIUM-MANGANESE-COPPER

by

Wentzle R. DeBoskey

Thesis submitted to the Graduate Faculty of the
Virginia Polytechnic Institute
in candidacy for the degree of

MASTER OF SCIENCE

in

Metallurgical Engineering

APPROVED:

Director of Graduate Studies

Dean of Engineering

APPROVED:

Head of Department

Supervisor or Major Professor

November 1955

Blacksburg, Virginia

TABLE OF CONTENTS

TABLE OF FIGURES

TABLE OF TABLES

ABSTRACT

The initial part of this investigation was to determine the ternary isothermal sections for the Cr-Co-Cu system and the Cr-Mn-Cu system at 1000°C. and 975°C., respectively. This was done by vacuum melting the Cr-Co-Cu alloys and annealing these alloys in an inert atmosphere of a helium-hydrogen gas mixture. The Cr-Mn-Cu alloys were melted under a helium atmosphere and annealed in evacuated Vycor tubes. By the use of metallographic techniques and x-ray analysis the phases present in each alloy were determined and the two ternary isothermal sections constructed.

It was found that copper had a very limited solid solubility in the sigma phase of both systems. The sigma field in the Cr-Co-Cu 1000°C. ternary isothermal comes into equilibrium with the terminal solid solutions of chromium, cobalt, and copper. In the Cr-Mn-Cu ternary isothermal section sigma comes into equilibrium with the terminal solid solution of chromium and cobalt and the face-centered cubic solid solution of copper in manganese. From these data the electron vacancy scheme[16] may not be extended to include copper due

to the limited solid solubility of copper in sigma. Also, the extent of copper solubility in the sigmas cannot be related to the solubility of the copper in cobalt or manganese.

INTRODUCTION

The most typical intermediate phase occurring in binary and ternary systems of the transition elements is the sigma phase, the first occurrence of which was reported by Bain and Griffiths[1] in the Fe-Cr system. Thereafter, sigma was reported in many other transition element systems, both ferrous and non-ferrous. Greenfield and Beck[2,3] have recently substantiated the occurrence of the sigma phase in a number of systems. These are listed according to the Period combination as follows:

First Period with First Period

V-Mn, V-Fe, V-Co, V-Ni, Cr-Mn, Cr-Fe, Cr-Co

Second Period with Second Period

Nb-Rh, Nb-Pd, Mo-Ru

Third Period with Third Period

Ta-Re, Ta-Pt, W-Re

First Period with Second Period

Cr-Ru, Mo-Mn, Mo-Fe, Mo-Co

First Period with Third Period

Cr-Re

Second Period with Third Period

Nb-Re, Nb-Pt, Mo-Re, Mo-Os, Ta-Rh

With reference to the First Long Period it is noted that sigma occurs only when either of the two transition elements to the left of manganese, vanadium or chromium, is combined with manganese or a transition element to the right of manganese. This combination of Groups VB, VIB, VIIB, and VIII also appears to hold both for the Second and Third Long Periods and the combinations of Long Periods.

The occurrence of sigma in twelve ternary systems was listed by Nevitt[4]. More recently, Darby, Greenfield, and Beck[5] substantiated the occurrence of sigma in eight more ternary systems. These twenty ternary systems are:

V-Fe-Co, V-Fe-Ni, V-Co-Ni, V-Mn-Fe, V-Mn-Co, V-Mn-Ni, V-Co-Cr, Cr-Co-Fe, Cr-Co-Mo, Cr-Co-W, V-Co-Mo, Cr-Fe-Mo, Cr-Fe-W, Cr-Fe-V, Cr-Mo-Ni, Cr-Ni-Fe, Cr-Ni-W, Cr-Fe-Ni, Cr-Fe-Si, Cr-Co-Ni.

Also, it was shown by Tucker[6] that the beta-uranium structure is analogous to that of sigma.

Sigma has been found to have a tetragonal lattice with thirty atoms per unit cell[7]. The very characteristic x-ray pattern gives an excellent method of rapid identification. This unique x-ray pattern is

common to all sigmas, although there is a slight parameter shift due to the different sized atoms involved.

Another spot-check means of identifying sigma, in some cases, is given by the non-magnetic room temperature behavior of sigma. It also was observed[8] and confirmed[9] that sigma becomes ferromagnetic around liquid air temperatures. Nevitt showed that low temperature ferromagnetism is a definite characteristic of the sigma phase.

Bain and Griffiths[1] along with their discovery of sigma observed the characteristic property of extreme hardness. This hardness causes severe embrittlement of alloys highly alloyed with transition elements when sigma is present. Thus, an understanding of the alloying behavior of the transition elements would lead to knowledge of the control of sigma.

THE REVIEW OF LITERATURE

The General Alloy Theory. In the general theory of alloys, one may classify the metallic elements as either transition elements or non-transition elements. The transition elements are characterized by having an electronic configuration of either 4s, 5s, or 6s electrons outside of partially filled d levels. The electronic configuration of the non-transition elements is that of valence electrons outside of filled levels.

Relationships developed by Hume-Rothery[10] can be used with fair reliability in predicting the alloying behavior of the non-transition elements. General predictions derivable from these relationships are as follows:

1. If the atomic diameters of the solvent and the solute atoms differ by more than about 15 per cent, the solid solubility range becomes small.
2. Large electro-chemical differences between the component metals give a tendency toward the formation of stable compounds rather than extensive terminal solid solutions.

3. The ratio of valence electrons to the number of atoms at ideal composition of many isomorphous compounds may correspond to one of the values, 3/2, 21/13, or 7/4, where the respective crystal structures becoming stable are body-centered cubic, complex cubic and close-packed hexagonal. The 3/2 ratio also tends to give rise to a beta-manganese, close-packed hexagonal type crystal structure.

Modifications of the above relationships must be made if predictions are to be made concerning the alloying behavior of a transition with a non-transition element. One modification requires that a zero valence be assigned to the transition element as pointed out by Cottrell[11] due to the necessity for filling the partially filled sub-bands of the transition elements. Raynor[12] has proposed a merger of Hume-Rothery's relationships with those of Pauling[13] as a further modification of the alloying behavior of a transition element with a non-transition element. In this modification a transition element of the First Long Period accepts enough electrons from the

structure to fill the Pauling non-bonding or atomic 3d sub-band while contributing no electrons of its own. This assumption gives rise to an electron-to-atom ratio of approximately 2.2 for isomorphous compounds of transition elements with aluminum.

When the alloying behavior of one transition element with another is investigated, Hume-Rothery's relationships show a low degree of applicability, especially in proposing critical electron-to-atom ratios. This electron-to-atom ratio would be a constant for combinations of the transition elements with one another if the postulation of Pauling is adopted that the number of bonding electrons remains constant, equal to 5.78 electrons across the First Long Period. This consideration, along with similarity of atomic diameters and electrochemical characteristics for these transition elements, gives rise to very low probability, by Hume-Rothery's relationships, that intermediate phases should exist.

The fact that the sigma phase, an exceptionally stable phase when certain conditions are present, occurs when certain transition elements are combined, gives rise to the consideration that factors, probably

of minor importance or even non-existent in non-transition elements, play a definite role in determining the alloying behavior of the transition elements.

The Sigma Phase. Dewey and Bain[14] were the first to suggest necessary conditions for the formation of the sigma phase. These conditions were that the atomic diameters must not differ by more than about 8 per cent and that the crystal structure of one of the component transition elements is body-centered cubic while the other component is face-centered cubic in at least one of its allotropic forms. The fact that sigma is found in the Mo-Ru binary system, where the crystal structures are body-centered cubic and hexagonal close-packed, respectively, shows that the latter is not a necessary condition. When sigma forms between elements in different Long Periods the atomic diameters of the component elements may differ by as much as 10 per cent. This fact eleminates the necessity of the first condition.

The proposal of Sully[15] and those of Beck[16] are dependent upon Pauling's theory of the transition elements of the First Long Period, which proposes that

metallic bonding is some form of covalent bonding. Pauling theorized that the transition elements have their d electrons sub-divided into two distinct groups, the atomic sub-group and the bonding sub-group. Pauling further postulated that the number of bonding electrons was constant across the First Transition Period from chromium to nickel. From magnetic saturation moment data Pauling inferred that a maximum of 4.88 electrons may enter into the atomic sub-group. Using this model, Sully correlated sigma to an electron-to-atom ratio of 2.25 which showed good agreement with the then existing data. Douglas[17] deduced and Heal and Silcock[18] confirmed through determinations of the volume of the first Brillouin zone from x-ray data that the electron-to-atom ratio for sigma with a filled Brillouin zone should be about 1.7. Because of these data, Sully modified his theory by eliminating the 0.66 4s electrons from taking part in the sigma bonding. This resulted in a modified electron-to-atom ratio for the sigma phase of about 1.7. This ratio for the sigma phase locates the mean composition of certain binary sigma phase fields in acceptable agreement with experimental data. Although acceptable agreement is

obtained, Sully's theory is hard to substantiate on any theoretical ground. For example, the ferromagnetic behavior of sigma shows that a full Brillouin zone, as proposed by Sully for his theory, is not correct. Even though there are weak points in the theory, one must give Sully credit for showing that sigma is at least partially electronic in its nature.

Independent of Sully, Beck and his co-workers[16] proposed a method of locating the composition of the sigma phase. Beck and co-workers noticed that the sigma phase fields of certain ternary systems seemed to follow constant electron vacancy lines. This electron vacancy, N_v, was derived from Pauling's theory and expressed by the following equation:

$$N_v = 4.88(V) + 4.66(Cr) + 3.66(Mn) + 2.66(Fe) + 1.71(Co) + 0.61(Ni)$$

where the chemical symbols stand for the atomic fraction of that particular element in the alloy. The numbers, 4.88 for vanadium, 4.66 for chromium, etc., are the Pauling values for the number of vacant atomic orbitals for the respective elements. To obtain closer agreement with existing data, vanadium's

vacancy number was increased to 5.66 when vanadium was combined with either cobalt or nickel. The vacancy number for manganese was lowered to 3.33 for closer agreement. These changes are partially explainable theoretically; but, inasmuch as Pauling's original theory was empirical in its origin, this proposal must remain a method for the location of the sigma phase, not a reason for the formation of sigma. Beck must be given credit, as was Sully, for showing that sigma is partially electronic in its nature. Beck and co-workers have found that the average N_v for sigma formed of elements of the First Long Period to be 3.41. Beck and co-workers have also found that molybdenum, a Group VI element of the Second Long Period, may be satisfactorily included in the proposal of locating the sigma phase field by assigning the vacancy number 4.66, that of chromium, to molybdenum. Beck and Greenfield[2] further found that any assignment of First Long Period vacancy numbers to elements of the Second and Third Long Periods was not feasible in that the location of the sigma phase field either was displaced or non-existent. This lack of consistency between Long Periods shows that the formation of sigma

is related to variables not yet clearly understood, and considerable further work will be required before a satisfactory theory for the sigma phase is developed.

OBJECT OF THE INVESTIGATION

The electron vacancy scheme for predicting the existence and location of the sigma phase holds rather nicely for combinations of First Long Period elements and is inadequate when extended to cover combinations of the Second and Third Long Periods. Another test of the range of applicability of the electron vacancy scheme would be to see whether the correlation leads to rational predictions about sigma formation when a zero vacancy number is assigned to a non-transition element such as copper in combination with a transition element such as chromium. By using the two elements, chromium and copper, with vacancy numbers of 4.66 and zero, respectively, a sigma may be postulated at a point 73.2 per cent chromium and 26.8 per cent copper by substitution into the N_v equation with N_v equal to 3.41. However, the chromium-copper binary system[19], Figure 1, page 23, shows that no sigma phase exists. However, the influence of a non-transition element on the stability of the sigma phase could still be studied by adding copper to a binary system such as Cr-Co or Cr-Mn, where the sigma phase is known

to exist, to determine the extent of solubility of copper in the sigma phase and to see if the boundaries of the sigma phase field follow the constant electron vacancy lines and point toward the hypothetical sigma point on the chromium-copper binary. Cobalt and manganese appeared to be logical choices for the third element because of the possibility of studying the effect of the solid solubility of copper in one of the component elements of the sigma-forming binary on the solid solubility of copper in sigma. Copper, as shown by the copper-cobalt binary system[20], Figure 2, page 24, has limited solid solubility in cobalt. Complete solid solubility at elevated temperatures is shown by the copper-manganese binary system[21], Figure 3, page 25. In both binary systems, Cr-Co[22] and Cr-Mn[23], sigma is stable at high temperatures so that equilibrium structures may be obtained without abnormally long annealing periods. The chromium-cobalt binary system, Figure 4, page 26, shows that sigma is stable at 1000°C. With copper having a melting point of 1083°C., the 1000°C. ternary isothermal section was chosen to be investigated since all components are solidified at this high temperature where sigma is stable. Because of an order-disorder transformation

at approximately 1000°C., shown in the chromium-manganese binary system, Figure 5, page 27, the 975°C. Cr-Mn-Cu ternary isothermal section was chosen to be investigated so that phase identification would be simplified.

Thus, in summary, the objects for this investigation are:

1. To determine the 1000°C. boundaries of the sigma phase in the two ternary systems Cr-Co-Cu and Cr-Mn-Cu.
2. To determine the phases which are in equilibrium with the sigma phase at 1000°C.
3. To determine whether the composition range of solubility of the sigma phases of the two ternary systems Cr-Co-Cu and Cr-Mn-Cu can be correlated with the distribution of d-shell electrons in the component transition and non-transition metals.
4. To determine whether the solubility of a non-transition metal in one of the component metals of the sigma phase affects the solubility of the non-transition metal in the sigma phase.

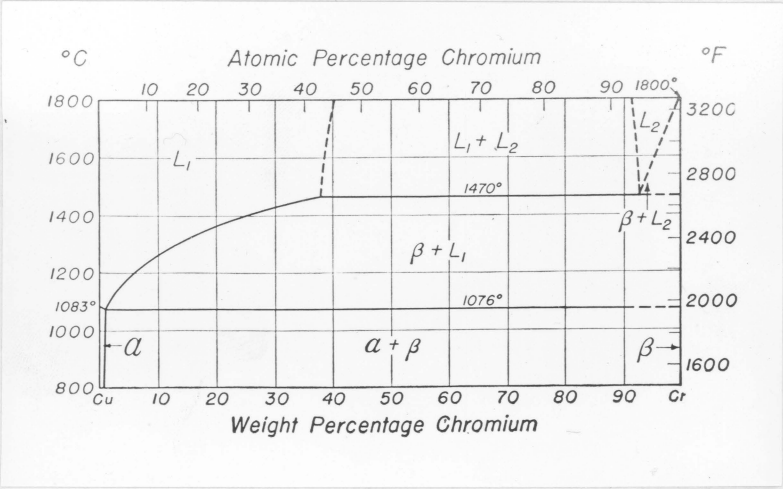

Figure 1. The Chromium-Copper Binary Diagram

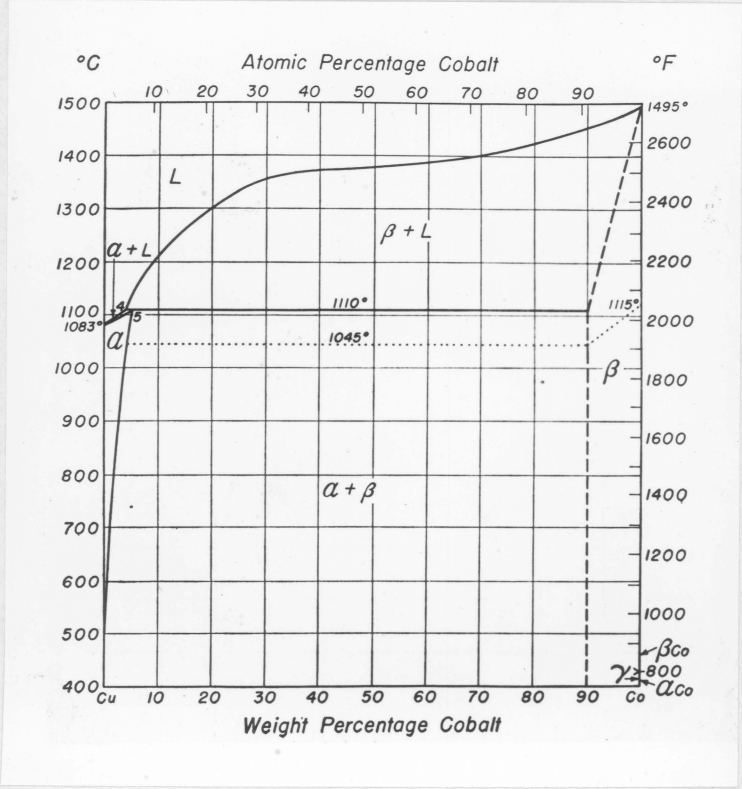

Figure 2. The Cobalt-Copper Binary Diagram

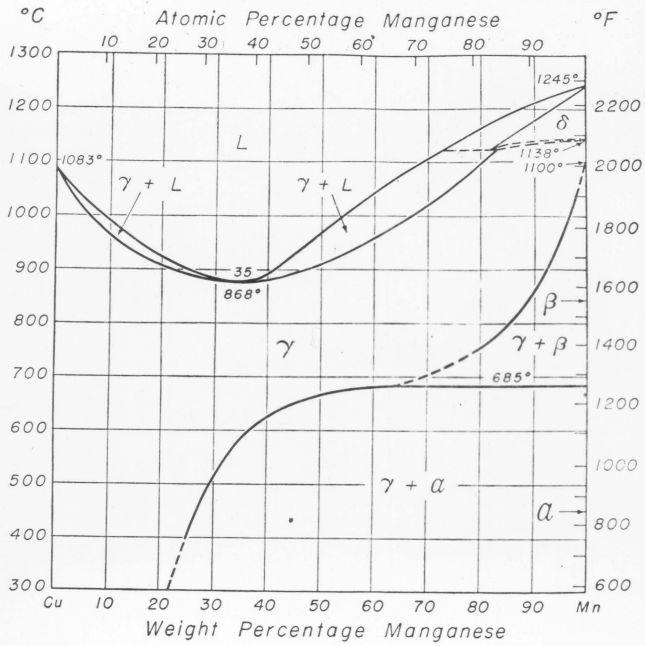

Figure 3. The Manganese-Copper Binary Diagram

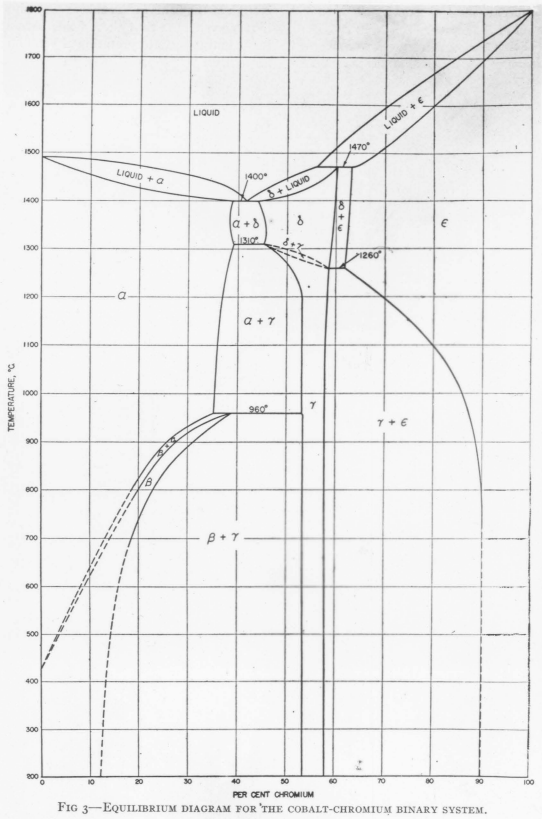

FIG 3—EQUILIBRIUM DIAGRAM FOR THE COBALT-CHROMIUM BINARY SYSTEM.

Figure 4. The Chromium-Cobalt Binary Diagram

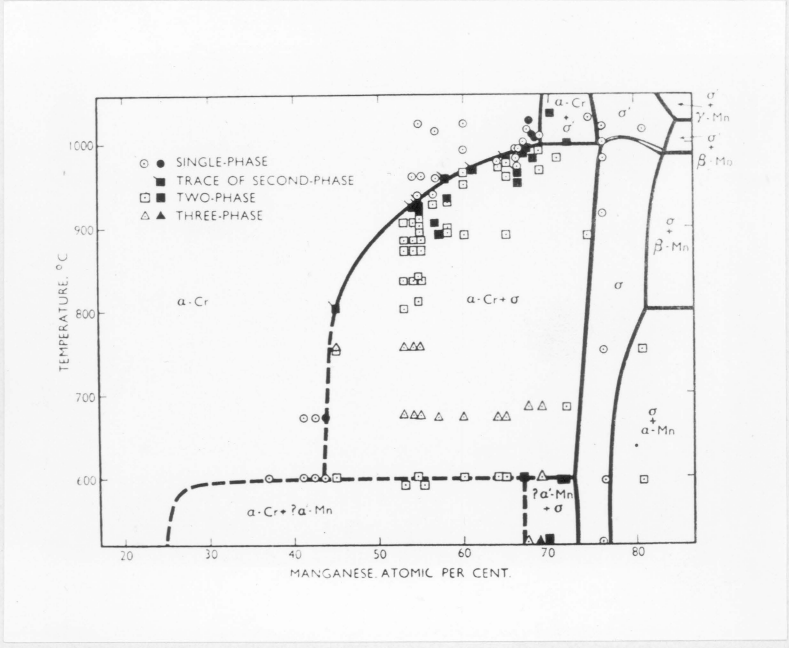

Figure 5. The Partial Chromium-Manganese Binary Diagram

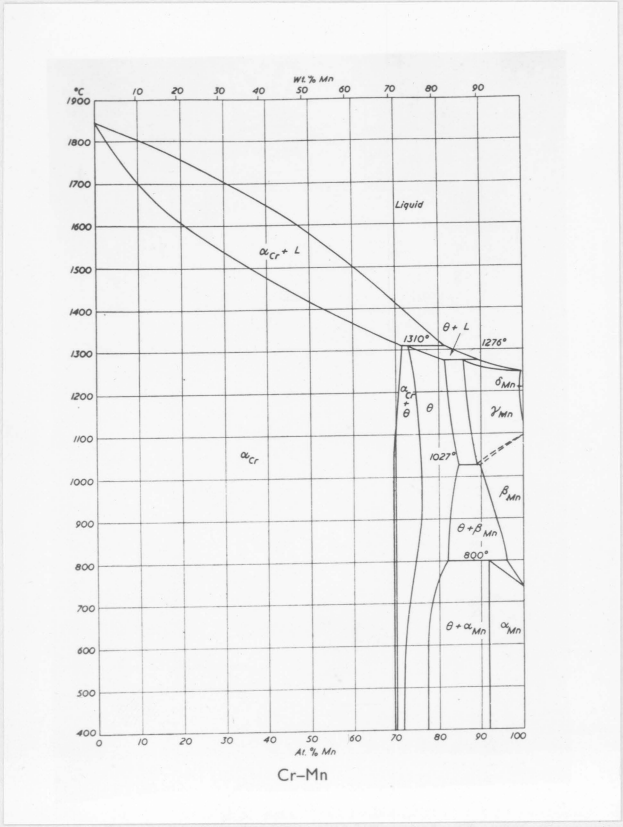

Cr–Mn

Figure 6. The Chromium-Manganese Binary Diagram

DESCRIPTION OF EQUIPMENT AND MATERIALS

Melting Furnace. All samples prepared were melted in a high-frequency induction furnace. See Figure 7, page 30. Power was supplied from a 20 kilowatt Ajax-Northrup mercury spark-gap converter. Maximum power dissipation used was approximately 15 kilowatts.

The induction furnace was a modified stationary cylindrical vacuum furnace, Model No. 313, produced by Ajax-Northrup. The induction coil arrangement, identical to the production model, consisted of a 42 turn water cooled copper coil, fourteen inches long and nine and one-fourth inches in diameter. Fitted inside of this coil was a fused silica tube, closed at one end, twenty-five inches in length and nine inches in diameter. This tube extended about seven and one-half inches above the top turn of the coil and was insulated from the coil by several wrappings of asbestos paper. Waxed to the open end of the silica tube was a steel flange. The finished top edge of the flange contained a groove into which an O-ring was fitted. To keep this O-ring seal cool during operation a thin sheet of copper was wrapped around the silica tube just

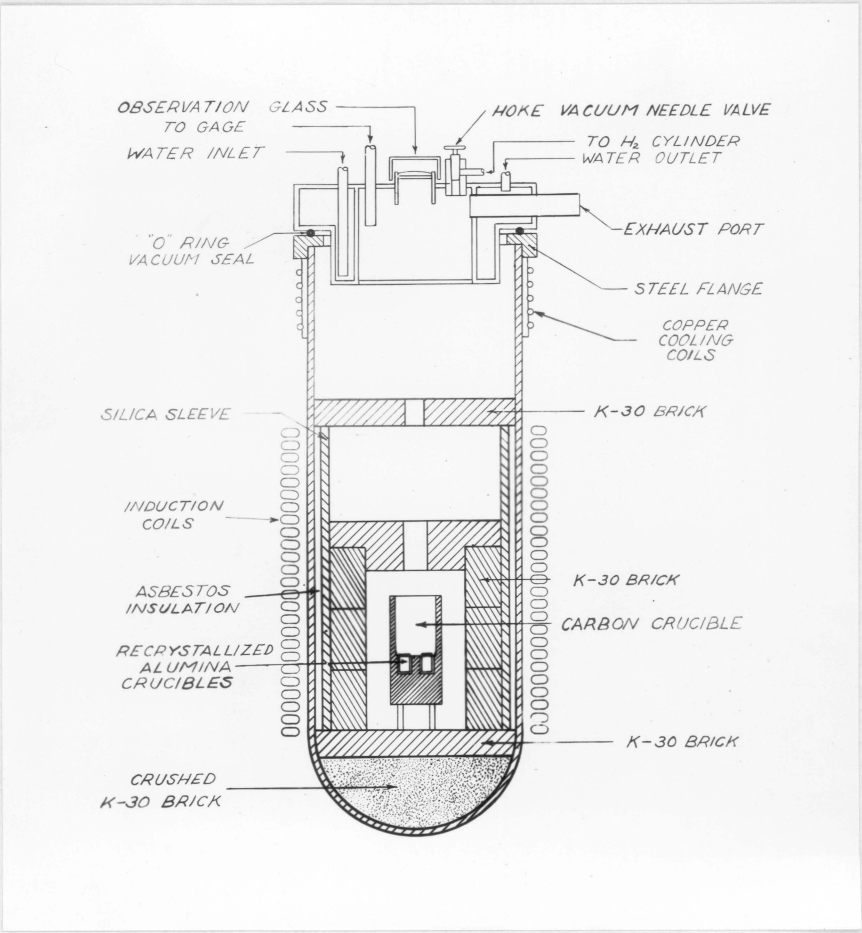

Figure 7. Schematic Diagram of the High-Frequency Induction Furnace

below the flange and several turns of copper tubing were soldered to the copper sleeve. Water was circulated for the cooling action.

The water-cooled steel top with a sight glass in the center which was supplied by Ajax-Northrup with the Model No. 313 furnace, was modified in several ways: First, the bottom surface was machined for better O-ring contact; second, the top was pierced by a one-fourth inch inside diameter brass tube which was brazed to the top and to which a Model No. 276AA McLeod type Stokes vacuum gauge was attached with heavy walled rubber tubing; third, a Hoke high vacuum needle valve was connected to the vacuum chamber through the top from a rubber tube which led to a supply of helium used in flushing out the system and for providing an inert atmosphere. This valve had a removable stem for venting the system to the atmosphere when necessary.

Inside and at the bottom of the silica tube were placed several inches of granulated K-30 brick to build up the test tube-like closed end of the tube to a flat surface. Upon this surface was placed a circle of K-30 brick of the appropriate diameter to act as the foundation for the rest of the internal build-up. A thin-

wall fused silica inner sleeve fourteen inches long and seven and seven-eighths inches in diameter was placed upon this base, the base being so located by the K-30 fill that the inner sleeve was positioned exactly inside the induction coil. Within the inner sleeve was a hollow cylinder about eight inches high and having a wall thickness of about one and one-half inches which was built with K-30 brick. This K-30 cylinder served as a radiation shield for the inner sleeve which in turn protected the silica tube. Additional radiation shields consisting of circles of K-30 brick cut to the appropriate diameter were positioned so as to rest on the top of the K-30 cylinder and on the top of the fused quartz inner sleeve.

Within the remaining space, cylindrical in shape, was placed a graphite heater crucible five inches long and two and one-half inches in diameter. Mounted on three three-sixteenths inch diameter carbon legs, this heater crucible was positioned so that a three-fourths inch spacing was obtained from the K-30 insulation in all directions. The carbon heater was bored out to a two inch depth, leaving a one-fourth inch wall. Three one inch holes, three-fourths inch deep were

triangularly positioned within this cup. High purity recrystallized alumina crucibles one and one-fourth inches long and seven-eighths inch in inside diameter were placed in these holes to serve as containers for the charges being melted.

Temperature measurements were obtained with a Pyro Model No. 85 optical pyrometer. The sight path to the charges in the melting crucibles was obtained by cutting holes in the two top radiation shields on a line from the sight glass in the steel top to the center of the heater crucible.

The system was connected by spring reinforced heavy walled vacuum tubing from the one and one-half inch exhaust port in the steel top to a Model 1397B Welch Duo-Seal mechanical vacuum pump. The pumping rate of this pump was two hundred and fifty liters per minute at five microns pressure.

Annealing Furnaces. The as-cast specimens, either bare or in evacuated and sealed Vycor tubes, were annealed in one or the other of two modified Model D-1-9 Burrell tube furnaces employing either an inert gas atmosphere of ninety-two per cent helium and eight per cent hydrogen or a vacuum of approximately two hundred

microns. Design of both furnaces was substantially the same.

The Burrell tube furnace, designed by the manufacturer to have two heating elements, was converted to a four element furnace with elements positioned at ninety degree intervals around the furnace tube. The heating elements used were three-eighths inch by ten inch Crystolon elements. Power to the series-connected elements was supplied from a two hundred and twenty volt main through mercury relays controlled by a Leeds and Northrup, Series H, controller-recorder and through a fifteen ampere variable transformer. The Leeds and Northrup controller responded to a platinum-platinum plus ten per cent rhodium thermocouple placed outside the furnace tube but adjacent to the annealing zone. With a controller temperature setting of T, the Leeds and Northrup controller, utilizing two off-on switches called for full power at temperatures below $T-\Delta T$, partial power from $T-\Delta T$ to $T+\Delta T$, and no power above $T+\Delta T$.

ΔT is determined by the setting of the two off-on switches. For this investigation ΔT was made as small as mechanically possible. Figure 8, page 36, shows

the circuit diagram for the furnace. Figure 9, page 37, shows the annealing furnaces. Power dissipation at an annealing temperature of 1000°C. at full power was approximately eleven hundred watts at ten amperes and at partial power approximately three hundred watts at five amperes. The annealing zone inside the tube, located about at the middle of the furnace, was approximately three inches long with a four degree centigrade temperature variation over the three inch length at annealing temperature. The temperature variation with time of annealing zone was dependent upon the controller characteristics. One furnace had a temperature variation with time of ± 2°C., the other ± 12°C. The majority of the specimens were annealed under the better conditions.

The vertically mounted furnace had a mullite McDanel combustion tube thirty inches long and one and three-fourths inches in inside diameter as its furnace tube. Brass flanges machined for O-rings were sealed on the ends of the tube with Apiezon W wax. A flat brass disc was bolted by brass bolts and wing nuts to the flange and drawn tight against the O-ring to achieve a seal. Piercing the copper discs at the

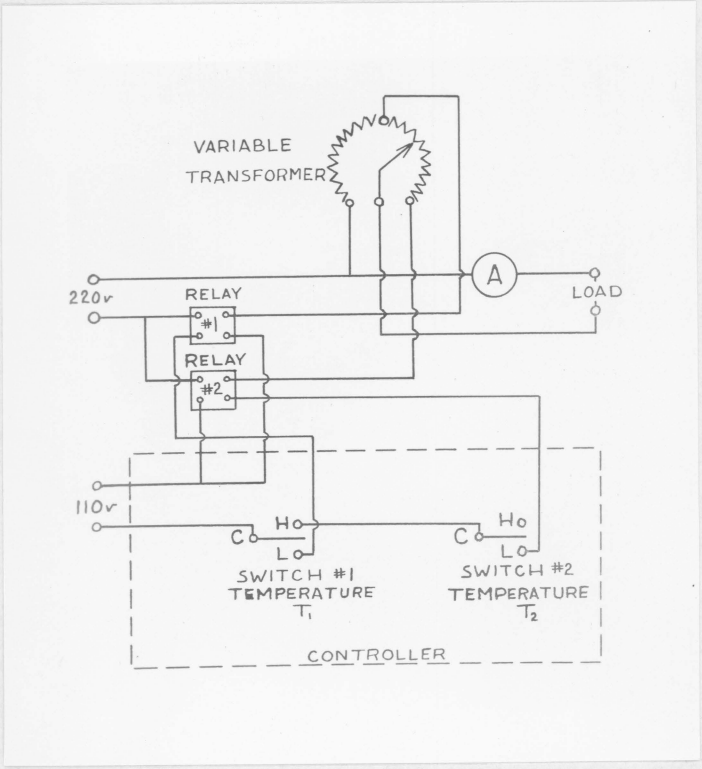

Figure 8. Circuit Diagram for the Annealing Furnaces

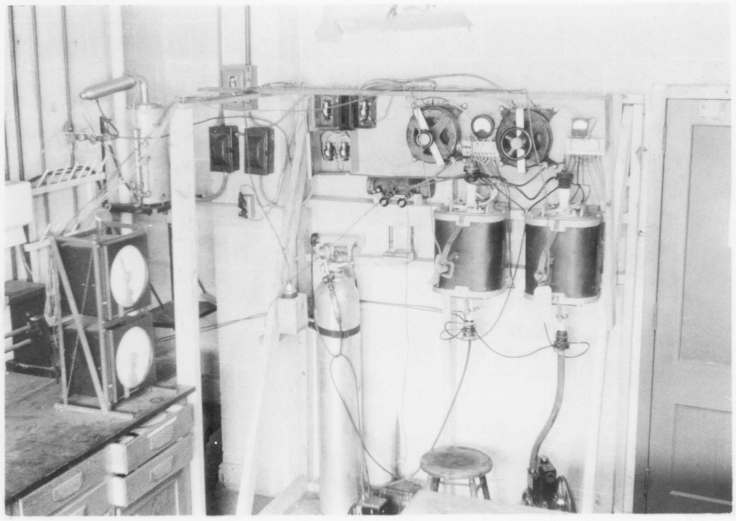

Figure 9. The Annealing Furnaces

top and bottom were short lengths of three-eighths inch diameter steel tubing which served as inlet and outlet ports, respectively, for the inert gas mixture. The upper tube ended in a tee fitting, the horizontal leg being either sealed off with a short length of rubber tube and a hose clamp for a vacuum or connected through a needle valve, a distribution manifold, a $CaSO_4$ desiccant column, a Deoxo catalytic purifier, and a pressure regulator to the helium-hydrogen gas cylinder when an inert gas atmosphere was employed. The vertical leg of the tee terminated with a short length of rubber tubing. A length of 0.032 inch diameter Kanthal wire was dropped through the rubber tubing and on the lower end of the wire the specimen was suspended in the annealing zone. A hose clamp sealed the rubber tube and held the Kanthal wire in position. When the annealing was done in the helium-hydrogen gas mixture the steel tubing emerging from the bottom disc was connected to an oil bath bubbler by means of which a qualitative measure of the rate of gas flow could be made. When vacuum annealing was employed this tube was connected to a vacuum pump.

Water was circulated through copper tubing soldered to the brass flanges to cool the ends of the furnace tube, the rubber O-ring, and the wax seal.

Materials. The alloy specimens prepared in this investigation were prepared from high purity metals. Analysis of these metals may be found in Table I, page 40.

Table I

Analysis of Component Metals by Weight Per Cent

	Electrolytic Manganese	Electrolytic Chromium	Electrolytic Copper Shot	Electrolytic Cobalt
Fe	0.001	0.06	0.0025	0.14
C	0.005	0.01		0.028
P	Not detectable			
Si	Trace			0.002
Cu		0.01	99.94-99.97	0.004
Mn	99.9 Min.			Nil
H_2	0.015	0.02		
O_2		0.45	0.02-0.55	
N_2		0.01		
Ni			0.0015	Trace
Al				0.008
As			0.0015	
Sb			0.0015	
Sulfide	0.018			
Sulfate	0.006			
Pb	0.005	0.005		Not detectable
Cr		99.00 Min.		
Co				Remainder
S		0.02	0.002	0.004
Ag			0.001	
Au			0.00001	

OPERATION OF EQUIPMENT

Melting Furnace. Thirty gram charges were prepared by weighing out the necessary quantities of the component metals to an accuracy of ± 0.05 gram. The charges were packed into recrystallized alumina crucibles, and these alumina melting crucibles were lowered into the wells of the graphite heater crucibles, three crucibles per run. The two K-30 brick radiation shields and the steel top were placed into their proper positions. With the top in position the system was evacuated to about five microns. A power of five kilowatts was then applied to the induction coils and held until the metal charge was outgassed. Power was then increased to ten to fifteen kilowatts. This increase in power raised the temperature of the charges to about 1500°C. in approximately twenty-five minutes, temperature being determined by use of the optical pyrometer. The system was flushed with high purity helium and re-evacuated periodically during the melting cycle. When the charges contained manganese the system was flooded with helium at 1100° and the remainder of the melting cycle finished with a helium atmosphere. After complete melting,

determined visually through the sight port in the top, the power was cut off and the charges allowed to cool below a red heat after being removed from the furnace.

The alumina crucibles in most cases were not attacked and could be reused four or five times for alloys in the same ternary system. Ingots were easily removed by inverting the crucible and tapping lightly. The ingots had smooth surfaces which were free from oxidation. All ingots were weighed upon removal from the alumina melting crucibles and any loss in weight recorded. The losses in weight were negligible for the Cr-Co-Cu system and about 0.6 gram per 30 gram charge in the Cr-Mn-Cu system.

Annealing Furnaces. The specimen for annealing consisted of approximately one-third of a one-eighth inch disc cut from the bottom of the thirty gram ingot. A wet cut-off wheel was used for the sectioning of the ingot.

A group of three specimens were wired together in an elongated cluster using Kanthal wire. The cluster was attached to a length of Kanthal wire and suspended in the furnace. Manganese-containing specimens were

individually sealed in evacuated ten mm. diameter Vycor tubes. Three Vycor tubes were bound together with Kanthal wire and supported in the furnace in the same manner as the bare specimens.

Prior to the anneal a chromel-alumel thermocouple was inserted down through the steel tube in the top fitting and the temperature of the annealing zone was determined with a Brown Model No. 1117 portable potentiometer. After the annealing zone temperature was stabilized at the desired point, the top brass disc was removed and the supporting Kanthal wire pushed up through the vertical leg of the tee. When an inert gas atmosphere was used the specimens were kept in the top of the furnace tube out of the high temperature zone until the air in the tube was replaced by the helium-hydrogen mixture. The air replacement was accomplished by flushing the tube with a moderate flow of the gas mixture for five to ten minutes. After flushing the gas flow was cut back until only a slightly positive pressure was obtained within the furnace tube, as indicated by the bubbler.

Specimens that were sealed in evacuated Vycor tubes were annealed utilizing a vacuum within the

furnace tube. The specimens were introduced into the furnace tube as before and were lowered slowly down into the annealing zone to prevent thermal shock to the Vycor tubes. After the specimens were in position the furnace tube was evacuated.

The anneal was for a duration of three or four days. This annealing time was determined by annealing the first specimens for several different time periods and comparing the annealed structure against the as-cast structure. It was assumed that the equilibrium structure had been attained when two successive checks of the microstructure did not show any further changes. After the specimens had been at the annealing temperature for the proper length of time, the bottom seal of the furnace tube was removed. Then the supporting Kanthal wire was severed and the specimens dropped into a container of cold tap water.

Phase Boundary Determinations. Approximately half of each of the annealed specimens was mounted in bakelite and prepared for metallographic examination. Polishing was done on a series of dry emery papers and the wet laps of 600 alundum on canvas and of Shamva on Beuhler Microcloth. Etching of the chromium-cobalt-

copper alloys was accomplished by using concentrated hydrochloric acid. The chromium-manganese-copper alloys were etched using 5 per cent Nital.

The mounted specimens were examined on a Bausch and Lomb Research Metallograph utilizing both bright field illumination and the phase contrast accessory. The determination of the phases present was done by comparing the phases in the specimens under examination with known phases in previous specimens.

The remainder of each of the annealed specimens was powdered to 250 mesh either by crushing or by filing. The powder was then spread on a glass slide using a rubber-base cement. This glass slide was mounted on a General Electric XRD-3 x-ray diffraction unit. This diffraction unit utilized unfiltered radiation from a chromium tube and a spectrogonimeter using a multi-chamber Geiger tube detector which automatically recorded the intensity of reflected radiation as a function the angle 2θ. The determination of the phases present was done by comparing the pattern of the specimens under examination with the patterns of known phases.

RESULTS AND DISCUSSION

Results. Approximately 25 per cent of the Cr-Co-Cu ternary system specimens were chemically analyzed. From these analyses the probable analysis for each specimen was determined by using the appropriate curves of Figure 10, page 47. Table II, page 48, lists the melt numbers, the proposed compositions, and the probable compositions. Also listed are the phases present in each specimen as determined by visual and by x-ray analysis. From Table II the partial ternary isothermal section at 1000°C., as shown in Figure 11, page 49, was drawn. This figure, which will be discussed in detail, shows that copper has a limited solubility in sigma. Also sigma is shown to come into equilibrium with the terminal solid solutions of chromium, cobalt, and copper. The copper phase being almost pure copper, as determined by x-ray analysis.

About 25 per cent of the Cr-Mn-Cu ternary system specimens were chemically analysed. From these chemical analyses the probable composition for each specimen was determined by using the appropriate curves of Figure 12, page 50. A list of the melt numbers, the proposed compositions, the probable compositions, and

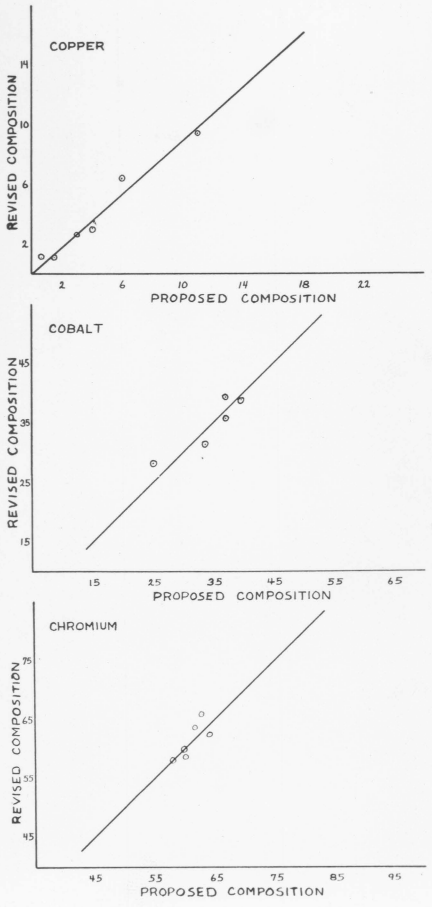

Figure 10. Curve of Proposed Analysis Versus Probable Analysis for the Component Elements of the Cr-Co-Cu Ternary System

Table II

The Chromium-Cobalt-Copper Alloys

Specimen No.	Proposed Composition atomic %	Revised Composition atomic %	Phases
9	59.1Cr 40.9Co	59.1Cr 40.9Co	γ
18	61.8Cr 37.2Co 1.0Cu	61.9Cr 37.3Co 0.8Cu	γ
19	60.8Cr 38.2Co 1.0Cu	60.9Cr 38.3Co 0.8Cu	γ
20	62.7Cr 34.3Co 3.0Cu	62.9Cr 34.4Co 2.7Cu	$\gamma+\alpha+\sigma$
21	61.7Cr 35.3Co 3.0Cu	61.9Cr 35.4Co 2.7Cu	$\gamma+\alpha+\sigma$
22	63.7Cr 31.3Co 5.0Cu	64.1Cr 31.5Co 4.4Cu	$\gamma+\alpha+\sigma$
23	62.7Cr 32.3Co 5.0Cu	63.1Cr 32.5Co 4.4Cu	$\gamma+\alpha+\sigma$
24	60.6Cr 34.4Co 5.0Cu	60.9Cr 34.6Co 4.4Cu	$\gamma+\alpha+\sigma$
25	64.0Cr 31.0Co 5.0Cu	64.4Cr 31.2Co 4.4Cu	$\gamma+\alpha+\sigma$
26	65.2Cr 25.8Co 9.0Cu	66.0Cr 26.1Co 7.9Cu	$\gamma+\alpha+\sigma$
27	64.0Cr 25.0Co 11.0Cu	64.9Cr 25.4Co 9.7Cu*	$\gamma+\alpha+\sigma$
28	68.0Cr 17.0Co 15.0Cu	69.2Cr 17.5Co 13.3Cu	$\gamma+\alpha+\sigma$
29	60.0Cr 37.0Co 3.0Cu	60.2Cr 37.1Co 2.7Cu*	$\gamma+\alpha+\sigma$
30	58.0Cr 39.0Co 3.0Cu	58.2Cr 39.1Co 2.7Cu	$\gamma+\epsilon+\sigma$
31	64.2Cr 32.8Co 3.0Cu	64.4Cr 32.9Co 2.7Cu	$\gamma+\alpha+\sigma$
32	66.0Cr 31.0Co 3.0Cu	66.2Cr 31.1Co 2.7Cu	$\gamma+\alpha+\sigma$
33	62.7Cr 33.3Co 4.0Cu	63.0Cr 33.4Co 3.6Cu*	$\gamma+\alpha+\sigma$
34	70.0Cr 27.0Co 3.0Cu	70.2Cr 27.1Co 2.7Cu	$\gamma+\alpha+\sigma$
35	48.0Cr 52.0Co	48.0Cr 52.0Co	$\gamma+\epsilon$
36	72.5Cr 37.5Co	72.5Cr 37.5Co	$\gamma+\alpha$
37	65.0Cr 34.0Co 1.0Cu	65.1Cr 34.1Co 0.8Cu	$\gamma+\alpha+\sigma$
38	61.5Cr 37.0Co 1.5Cu	61.6Cr 37.1Co 1.3Cu*	$\gamma+\alpha+\sigma$
39	62.3Cr 37.0Co 0.7Cu	62.4Cr 37.0Co 0.6Cu	$\gamma+\alpha+\sigma$
40	59.8Cr 39.6Co 0.6Cu	59.9Cr 39.6Co 0.5Cu*	$\gamma+\epsilon+\sigma$
43	59.0Cr 35.0Co 6.0Cu	59.4Cr 35.3Co 5.3Cu	$\gamma+\alpha+\sigma$
44	58.0Cr 36.0Co 6.0Cu	58.4Cr 36.3Co 5.3Cu*	$\gamma+\alpha+\sigma$
45	57.0Cr 37.0Co 6.0Cu	57.4Cr 37.3Co 5.3Cu	$\gamma+\sigma$

* Chemically analyzed.

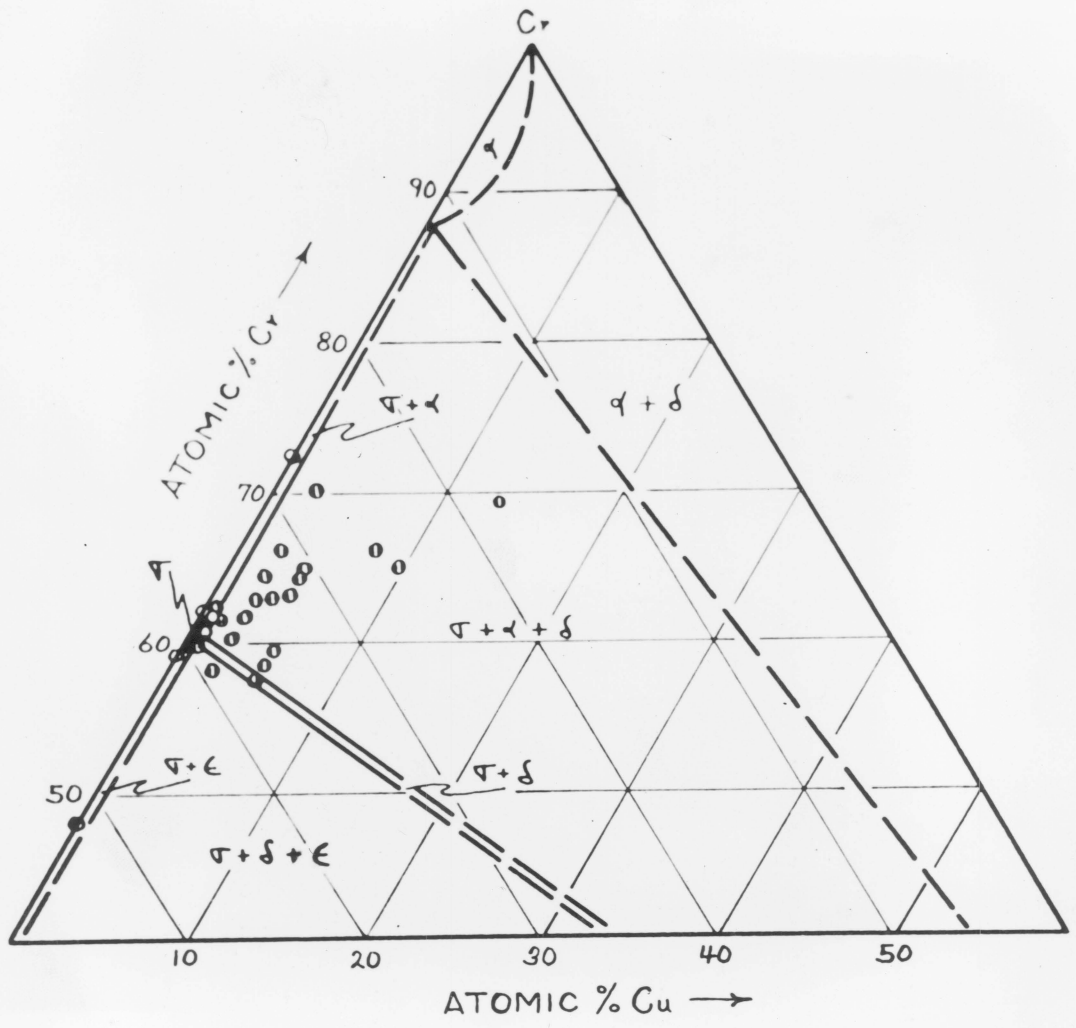

Figure 11. The Partial Cr-Co-Cu Ternary Isothermal Section at 1000°C.

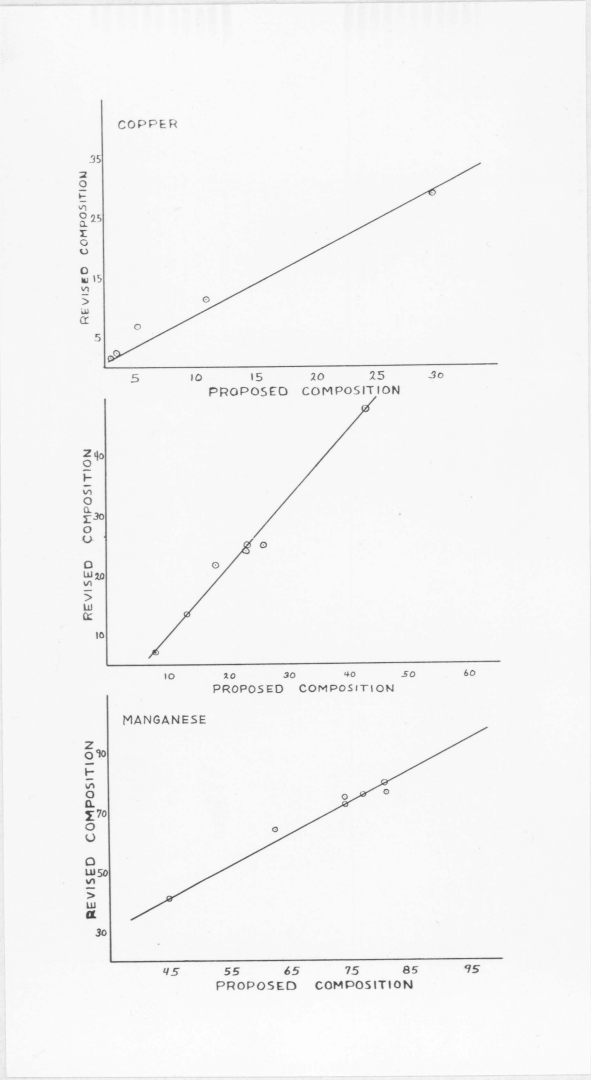

Figure 12. Curve of Proposed Analysis Versus Probable Analysis for the Component Elements of the Cr-Mn-Cu Ternary System

the phases present in each specimen may be found in Table III, page 52. From Table III the partial ternary isothermal section at 975°C., as shown in Figure 13, page 53, was drawn. This figure also shows that copper has a limited solubility in sigma. Sigma is shown also to be in equilibrium with the chromium terminal solid solution, the beta-manganese terminal solid solution, and the manganese-rich solid solution of manganese and copper. Sigma does not come into equilibrium with the liquid or the copper-rich solid solution of manganese and copper in the copper corner of the ternary isothermal.

Discussion of Results. The sigma phase boundary in the Cr-Co-Cu ternary system was determined by the existence of very small quantities of the terminal solid solutions in specimens 38, 39, and 40. X-ray analysis did not substantiate their presence due to the small quantities present. From the Cr-Co binary diagram, Figure 4, page 26, the limit of the solid solubility of cobalt in chromium was found to be 12.5 per cent cobalt. From this information and the fact that chromium shows no solid solubility for copper, as shown in Figure 1, page 23, the alpha chromium or chromium terminal solid

Table III

The Chromium-Manganese-Copper Alloys

Specimen No.	Proposed Composition atomic %	Revised Composition atomic %	Phases
101	80.0Mn 20.0Cr	78.5Mn 21.1Cr	γ
102B	74.0Mn 25.9Cr	70.5Mn 29.5Cr*	γ
103	86.0Mn 14.0Cr	84.6Mn 14.3Cr	$\gamma + \beta$
104	68.2Mn 27.8Cr 4.0Cu	66.8Mn 29.4Cr 4.4Cu	$\gamma + \alpha + \gamma$
105	56.4Mn 35.6Cr 8.0Cu	54.9Mn 37.8Cr 8.2Cu	$\gamma + \alpha$
106	44.8Mn 43.2Cr 12.0Cu	41.2Mn 47.4Cr 11.4Cu*	$\gamma + \alpha$
107	77.0Mn 22.0Cr 1.0Cu	75.6Mn 23.0Cr 1.5Cu	γ
108	74.2Mn 23.8Cr 2.0Cu	72.5Mn 25.2Cr 2.3Cu*	$\gamma + \alpha + \gamma$
109	71.2Mn 25.8Cr 3.0Cu	69.6Mn 27.2Cr 3.4Cu	$\gamma + \alpha + \gamma$
110	66.0Mn 34.0Cr	64.5Mn 36.0Cr	$\beta + \alpha$
111	100Mn	100Mn	
115	70.6Mn 22.1Cr 7.4Cu	69.1Mn 23.0Cr 7.6Cu	$\gamma + \alpha + \gamma$
116	59.5Mn 29.7Cr 11.2Cu	57.9Mn 31.2Cr 11.3Cu	$\gamma + \alpha + \gamma$
117	77.4Mn 17.1Cr 5.6Cu	76.0Mn 17.6Cr 5.9Cu	$\gamma + \alpha + \gamma$
119	81.9Mn 18.1Cr 1.1Cu	76.5Mn 21.6Cr 1.9Cu*	$\gamma + \beta$
120	62.5Mn 19.8Cr 17.8C8	61.0Mn 20.7Cr 17.8Cu	$\alpha + \gamma + L$
121	50.4Mn 20.1Cr 29.6Cu	48.4Mn 21.0Cr 28.8Cu	$\alpha + \gamma + L$
122	62.5Mn 7.9Cr 29.6Cu	64.0Mn 7.2Cr 28.8Cu*	$\alpha + \gamma + L$
123B	71.2Mn 28.8Cr	69.6Mn 30.5Cr	$\gamma + \alpha$
124B	75.1Mn 24.9Cr	73.6Mn 26.2Cr	γ
125B	77.0Mn 23.0Cr	76.1Mn 23.9Cr*	γ
126	84.5Mn 11.8Cr 3.9Cu	83.0Mn 11.9Cr 4.3Cu	$\gamma + \beta + \gamma$
127	76.4Mn 11.8Cr 11.8Cu	75.0Mn 11.9Cr 11.9Cu	$\gamma + \alpha + \gamma$
128	92.1Mn 3.9Cr 3.9Cu	90.6Mn 3.1Cr 4.3Cu	$\beta + \gamma$
129	50.0Mn 30.0Cr 20.0Cu	48.0Mn 31.8Cr 19.7Cu	$\alpha + \gamma + L$
130	44.0Mn 30.0Cr 26.0Cu	42.0Mn 31.8Cr 25.5Cu	$\alpha + \gamma + L$
132	83.0Mn 11.0Cr 6.0Cu	81.5Mn 11.5Cr 6.4Cu	$\gamma + \alpha + \gamma$
133	84.0Mn 8.0Cr 8.0Cu	82.3Mn 8.1Cr 8.3Cu	$\gamma + \alpha + \gamma$
134	80.0Mn 9.0Cr 11.0Cu	78.5Mn 9.1Cr 11.3Cu	$\gamma + \alpha + \gamma$

* Chemically analyzed.

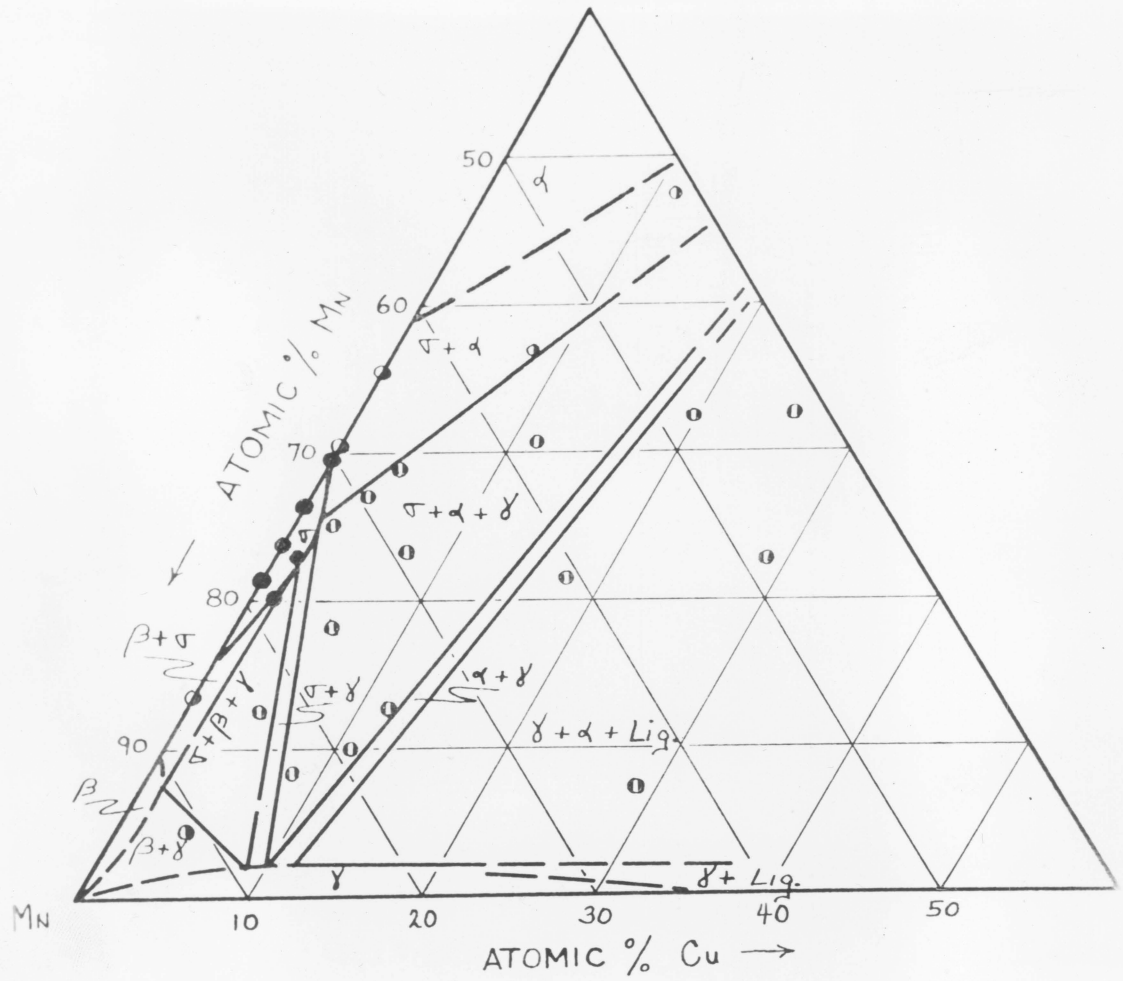

Figure 13. The Partial Cr-Mn-Cu Ternary Isothermal Section at 975°C.

solution boundary was drawn in speculatively. From similar data from the Cr-Co binary diagram and Co-Cu binary diagram, the cobalt terminal solid solution, the epsilon phase, is shown to extend from 39 per cent chromium on the Cr-Co binary to 9 per cent copper on the Co-Cu binary. Specimens 37 and 40 show, by the presence of a small amount of the copper terminal solid solution, the delta phase, that the two phase regions of sigma plus alpha and sigma plus epsilon are very narrow, indicating that copper has limited solubility in the alpha and epsilon phases when they are in a two phase equilibrium with sigma. Sigma in this ternary isothermal section is also in a two phase equilibrium with the delta copper phase. This delta phase is almost pure copper since copper shows very little solubility for either cobalt or chromium. The x-ray analysis gave d values for this delta phase very close to those of pure copper. The two phase sigma plus delta corridor is very narrow, which is indicated by the presence of small quantities of the third phase, either alpha or epsilon, in specimens straddling a line drawn between the mean sigma position on the Cr-Co binary diagram to the copper corner.

Specimen 45 did not exhibit the presence of a third phase, indicating that it lay within the two phase corridor. The phase boundaries in the region of the sigma field are fairly well established by the visual estimates of the amounts of the phases present. The spots where the boundary konodes of the two phase regions meet at a single phase region can be the only place where a three phase region may touch a single phase region. This fact, together with the knowledge that the delta phase is almost pure copper, indicates that the boundaries of the two three-phase triangles, shown by dashed lines on the isothermal section, are probably correct.

Specimens 38, 39, and 40 were also annealed at 1100°C. Several specimens were also annealed at 900°C. These specimens, when examined microscopically, showed the presence of the same phases in the same relative amounts as did the specimens annealed at 1000°C. This indicates that the equilibrium between the phases present did not change appreciably on raising or lowering the temperature.

The sigma phase boundary in the Cr-Mn-Cu ternary system was determined by the existence of very small

quantities of other phases in specimens 108 and 119. The sigma will take into solid solution only a small amount of copper, as shown by specimens 107 and 108. The sigma phase field in the Cr-Mn binary system was found to extend between 70.5 atom per cent manganese and 84 atom per cent manganese, rather than the 76 to 84 atom per cent manganese as shown in Figures 5 and 6, pages 27 and 28. It was noted that there was some dispute as to the location of the limit of manganese solid solubility in chromium between the binary diagram in the Metals Reference Book[24], Figure 6, and that of Pearson and Hume-Rothery, Figure 5. Specimen 110, which exhibits approximately equal amounts of the two phases, sigma and alpha, shows that the latter diagram is probably correct with regard to the solid solubility limit. The chromium terminal solid solution boundary was again drawn in speculatively, from a consideration of the binary diagrams. From Figure 13, page 53, the solid solubility of chromium in beta-manganese was found to be 9.5 atom per cent. From this observation and the fact that beta-manganese shows no solid solubility for copper, as shown in Figure 6, the beta-manganese terminal solid solution

boundary could be drawn in speculatively. The presence of a very small amount of beta in specimen 119 shows that the two phase region of sigma plus beta is very narrow, indicating that copper has a very low solid solubility in these two phases when they are in a two phase equilibrium. The boundary between the two phase region of alpha plus sigma and the three phase region of sigma plus alpha plus gamma was easily established due to the presence of very small quantities of gamma in specimens 108, 109, and 104, plus the absence of the gamma phase in specimens 105 and 106.

The gamma phase field, a face centered cubic solid solution of copper in manganese on the Cu-Mn binary diagram, probably comes into equilibrium with sigma and alpha as shown in Figure 13, page 53, since specimens 132 and 134 are sigma and specimens 128, 126, 132, and 127 exhibit visually small amounts of either beta, sigma, or alpha. It was noted that the gamma phase could not be entirely retained by quenching from the annealing temperature. This being due, probably, to not enough copper being present to stabilize the face-centered cubic manganese. The phase boundaries are fairly well established by the visual estimates of

the amounts of the phases present. The three phase triangle of sigma plus alpha plus gamma is well established due to these visual estimates. Specimens 120, 129, 130, 121, and 122 showed definite signs of melting at the annealing temperature and when examined visually showed a typical cored structure due to rapid solidification during the quenching operation. The approximate position of the three phase triangle as shown by the dashed lines of gamma plus alpha plus liquid was established by the visual estimates of the amounts of liquid present at the annealing temperature of 975°C.

The very low solid solubility of copper in the sigma phase of either the Cr-Co binary system or the Cr-Mn binary system gives insufficient data as to whether the electron vacancy scheme can be extended to copper by assigning copper a zero electron vacancy number. In the only other case of a non-transition element being combined with sigma, the Fe-Cr-Si system[25], sigma was shown to have a solid solubility for silicon of about 15 per cent at 1000°C. This would seem to indicate that the greater the number of valence electrons the non-transition element has, the

greater is its solubility in sigma. Thus, the solid solubility of the non-transition element in sigma appears to be governed by electronic considerations.

The relative solubility of copper in cobalt and manganese seems to have no effect on the solubility of copper in sigma. It would seem, therefore, that the low solubility of copper in chromium is what inhibits the solubility of copper in sigma. The other non-transition element for which the solubility has been determined in a sigma, silicon, shows a solubility in chromium of 7.5 per cent[26]. This, plus the fact that silicon is soluble in the Fe-Cr sigma to about 15 per cent, suggests that if the non-transition element is soluble in chromium, then it will be soluble in sigma formed with that element. Further investigation will be necessary to substantiate the validity of this generalization.

Photomicrographs.

Specimen 101. This is a photomicrograph of an all sigma alloy in the Cr-Mn binary system. The light gray structure is sigma which is broken up by the many cracks and voids which appear black.

Specimen 103. This is a two phase structure of sigma and beta-manganese. The beta-manganese is cut through with twin bands due to the transformation which occurs in quenching from the annealing temperature.

Specimen 106. This shows the two phase equilibrium between sigma and alpha-chromium. The light areas are sigma with the gray areas between being a mechanical mixture of sigma and alpha. The black areas are voids.

Specimen 115. This photomicrograph shows the three phase equilibrium between sigma, alpha-chromium, and gamma-manganese-copper. The light areas are sigma, the homogeneous gray areas are gamma, and the mottled gray areas are alpha.

Specimen 35. This shows the two phase equilibrium between sigma and epsilon-cobalt in the Cr-Co binary system. The lighter areas are the epsilon in the matrix of light gray sigma. The black areas are either voids or cracks.

Specimen 36. This shows the two phase equilibrium between sigma and alpha-chromium in the Cr-Co

binary system. The light areas are sigma and the darker gray areas are alpha.

Specimen 28U. This is a photomicrograph of an unetched three phase alloy in the Cr-Co-Cu ternary system. The copper, the dark gray areas, and the background, with appears to be all sigma, is all that is visible. The black areas show the presence of a tramp phase, an inclusion.

Specimen 28E. This is a photomicrograph of Specimen 28U etched. The background of 28U can now be resolved into two phases, sigma and alpha. The small grains are alpha in a matrix of sigma. Grain orientation has caused the specimen to etch unevenly.

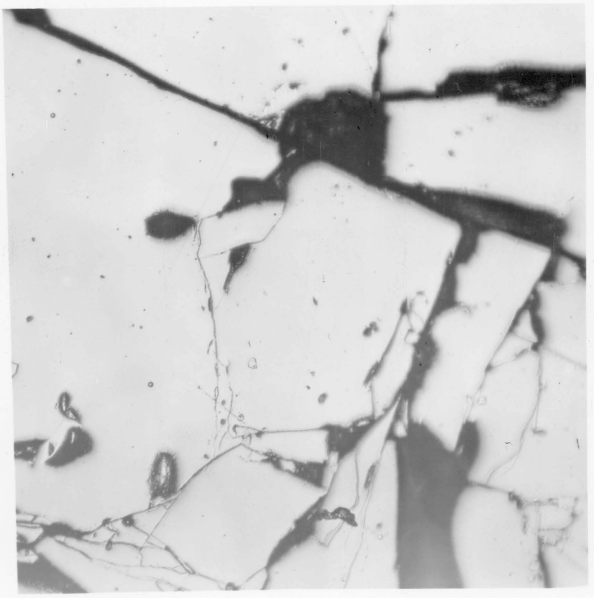

Figure 14. Photomicrograph of Specimen 101

Figure 15. Photomicrograph of Specimen 103

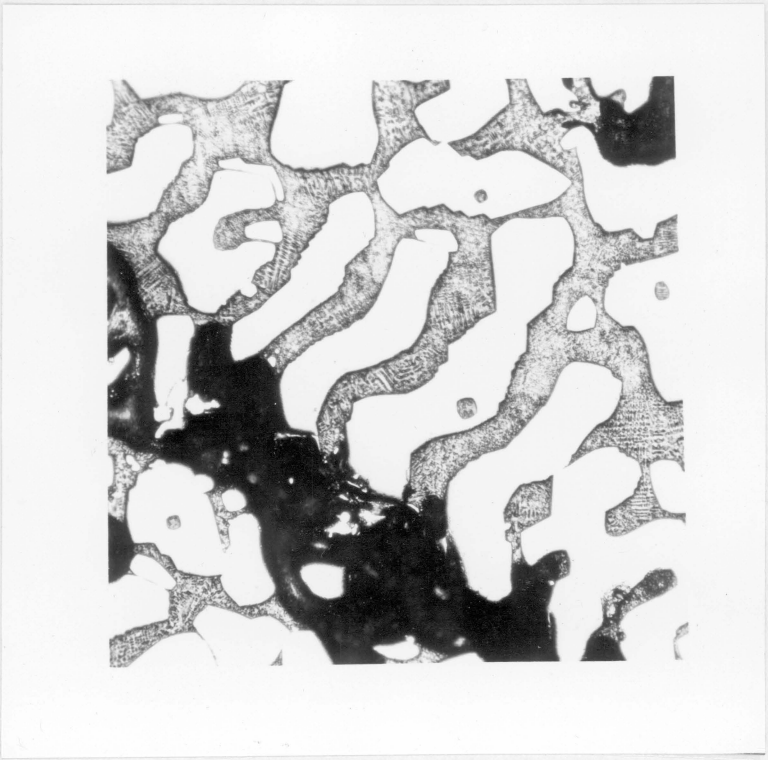

Figure 16. Photomicrograph of Specimen 106

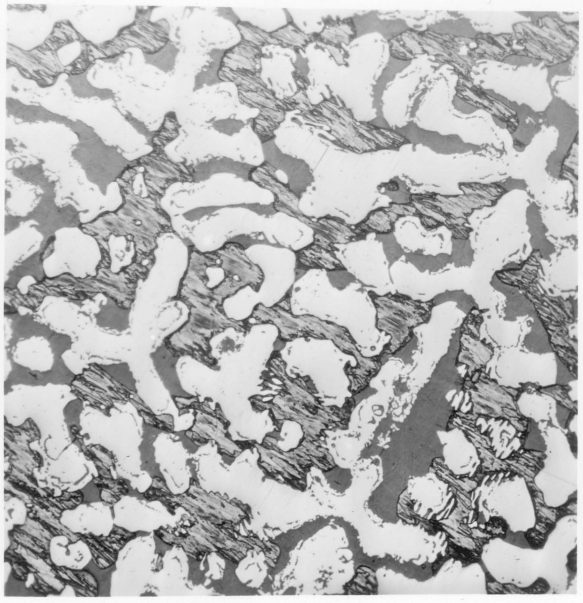

Figure 17. Photomicrograph of Specimen 115

Figure 18. Photomicrograph of Specimen 35

Figure 19. Photomicrograph of Specimen 36

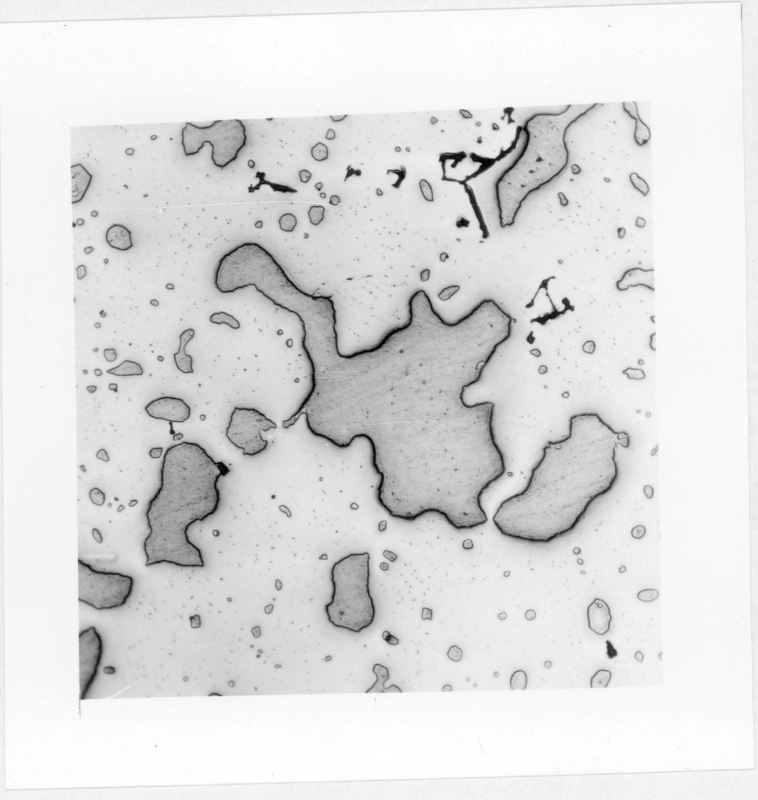

Figure 20. Photomicrograph of Specimen 28U

Figure 21. Photomicrograph of Specimen 28E

CONCLUSIONS

The conclusions of this investigation may be summarized as follows:

1. Sigma comes into equilibrium with the three terminal solid solutions of chromium, cobalt, and copper in the Cr-Co-Cu ternary system and the terminal solid solutions of manganese and chromium plus the face-centered cubic solid solution of copper in manganese in the Cr-Mn-Cu ternary system.
2. The electron vacancy scheme may not be extended to include copper due to the very low solid solubility of copper in the sigmas of the Cr-Co and Cr-Mn binary systems.
3. The extent of solid solubility of copper in the two sigma phases investigated cannot be related to the relative solubilities of copper in cobalt and manganese.

SUMMARY

During this investigation ternary isothermal sections for the Cr-Co-Cu system and the Cr-Mn-Cu system were determined. It was found that copper had a very low solubility in the sigma phase in both systems. The sigma field in the 1000°C. isothermal section of the Cr-Co-Cu system was in equilibrium with the terminal solid solutions in the chromium corner, the cobalt corner, and the copper corner. In the 975°C. isothermal section of the Cr-Mn-Cu system the sigma field was in equilibrium with the terminal solid solutions in the chromium and manganese corners and with the face-centered cubic solid solution of copper in manganese.

ACKNOWLEDGMENTS

The author wishes to express his sincere appreciation to Professor Michael V. Nevitt, Head, Department of Metallurgical Engineering, Virginia Polytechnic Institute, who gave the author competent assistance, frequent encouragement, and worthy advice.

The National Science Foundation provided the financial support for this investigation. This support is gratefully acknowledged.

To Professor Charles I. Rich, Department of Agronomy, thanks are expressed for his instruction and assistance in the use of the General Electric XRD-3 x-ray diffraction unit.

The Electro Manganese Corporation provided the high purity electrolytic manganese used in this investigation.

The author wishes to acknowledge the encouragement given him by other members of the teaching staff of the Virginia Polytechnic Institute.

REFERENCES

1. E. C. Bain and W. E. Griffiths, Trans. AIME (1927), 75, 166.

2. P. Greenfield and P. A. Beck, "Intermediate Phases in Binary Systems of Certain Transition Elements," to be published.

3. P. Greenfield and P. A. Beck, Trans. AIME (1954), 200, 253.

4. M. V. Nevitt, "Curie Temperatures of Binary and Ternary Sigma Phases," Doctorate Thesis, University of Illinois (1954).

5. J. B. Darby, P. Greenfield, and P. A. Beck, "The Sigma Phase in Certain Ternary Systems with Vanadium."

6. C. W. Tucker, Science (1950), 112, 448.

7. B. G. Bergman and D. P. Shoemaker, Jnl. Chem. Phys. (1951), 19, 515; also, Jnl. Am. Chem. Soc. (1950), 72, 5793.

8. K. W. J. Bowen and J. P. Hoar, Research (1950), 3, 484.

9. P. A. Beck, Trans. AIME (1952), 194, 420.

10. W. Hume-Rothery, "Atomic Theory for Students of Metallurgy," Inst. of Metals, London (1946).

11. A. H. Cottrell, "Theoretical Structural Metallurgy," Edward Arnold and Co., London (1948).

12. G. V. Raynor and P. C. Pfiel, Jnl. Inst. Met. (1947), 73, 397.

13. L. Pauling, Phys. Rev. (1938), 80, 173.

14. P. Duwez and S. R. Bain, Proc. ASTM (1950), 50.

15. A. H. Sully, Jnl. Inst. Met. (1951), 80, 173.

16. S. Rideout, W. D. Manly, E. L. Kamen, B. S. Lement, and P. A. Beck, Trans. AIME (1949), 191, 872.

17. A. M. B. Douglas, Brit. J. Appl. Phys. (1951), 2, 305.

18. T. J. Heal and J. M. Silcock, ibid.

19. ASM Handbook, 1948 Edition, 1193.

20. ASM Handbook, 1948 Edition, 1191.

21. ASM Handbook, 1948 Edition, 1198.

22. AIME Trans. (1949), 180, 579.

23. W. B. Pearson and W. Hume-Rothery, Jnl. Inst. Met. (1952-53), 81, 311.

24. Metals Reference Book, Vol. 1, 373.

25. A. G. H. Anderson and E. R. Jette, Trans. ASM (1936), 24, 375.

26. ASM Handbook, 1948 Edition, 1195.

The vita has been removed from the scanned document